entropy

MDPI

Article

Non-Thermal Quantum Engine in Transmon Qubits

Cleverson Cherubim [1,*], Frederico Brito [1] and Sebastian Deffner [2]

[1] Instituto de Física de São Carlos, Universidade de São Paulo, C.P. 369, 13560-970 São Carlos, SP, Brazil; fbb@ifsc.usp.br

[2] Department of Physics, University of Maryland Baltimore County, Baltimore, MD 21250, USA; deffner@umbc.edu

* Correspondence: cleverson.cherubim@usp.br

Received: 8 May 2019; Accepted: 27 May 2019; Published: 29 May 2019

Abstract: The design and implementation of quantum technologies necessitates the understanding of thermodynamic processes in the quantum domain. In stark contrast to macroscopic thermodynamics, at the quantum scale processes generically operate far from equilibrium and are governed by fluctuations. Thus, experimental insight and empirical findings are indispensable in developing a comprehensive framework. To this end, we theoretically propose an experimentally realistic quantum engine that uses transmon qubits as working substance. We solve the dynamics analytically and calculate its efficiency.

Keywords: quantum heat engines; quantum thermodynamics; nonequilibrium systems

1. Introduction

Recent advances in nano and quantum technology will necessitate the development of a comprehensive framework for *quantum thermodynamics* [1]. In particular, it will be crucial to investigate whether and how the laws of thermodynamics apply to small systems, whose dynamics are governed by fluctuations and which generically operate far from thermal equilibrium. In addition, it has already been recognized that at the nanoscale many standard assumptions of classical statistical mechanics and thermodynamics are no longer justified and even in equilibrium quantum subsystems are generically not well-described by a Maxwell-Boltzmann distribution, or rather a Gibbs state [2]. Thus, the formulation of the statements of quantum thermodynamics have to be carefully re-formulated to account for potential quantum effects in, for instance, the efficiency of heat engines [3–6].

In good old thermodynamic tradition, however, this conceptual work needs to be guided by experimental insight and empirical findings. To this end, a cornerstone of quantum thermodynamics has been the description of the working principles of quantum heat engines [7–17].

However, to date it is not unambiguously clear whether quantum features can always be exploited to outperform classical engines, since to describe the thermodynamics of non-thermal states one needs to consider different perspectives—different than the one established for equilibrium thermodynamics. For instance, it has been shown that the Carnot efficiency cannot be beaten [4,18] if one accounts for the energy necessary to maintain the non-thermal stationary state [19–22]. However, it has also been argued that Carnot's limit can be overcome, if one carefully separates the "heat" absorbed from the environment into two different types of energy exchange [23,24]: one is associated with a variation in *passive energy* [25,26] which would be the part responsible for changes in entropy, and the other type is a variation in *ergotropy*, a work-like energy that could be extracted by means of a suitable unitary transformation. On the other hand, it has been shown [27] that a complete thermodynamic description in terms of *ergotropy* is also not always well suited. Having several perspectives to explain the same phenomenon is a clear indication of the subtleties and challenges faced by quantum thermodynamics,

and which can only be settled by the execution of purposefully designed experiments. Therefore, theoretical proposals for feasible and relevant experiments appear instrumental.

In this work we propose an experiment to implement a thermodynamic engine with a transmon qubit as the working substance (WS), which interacts with a non-thermal environment composed by two subsystems, an externally excited cavity (a superconducting transmission line) and a classical heat bath [28] with temperature T. The WS undergoes a non-conventional cycle (different from Otto, Carnot, etc.) [29] through a succession of non-thermal stationary states obtained by slowly varying its bare energy gap (frequency) and the amplitude of the pumping field applied to the cavity. We calculate the efficiency of this engine for a range of experimentally accessible parameters [28,30–32], obtaining a maximum value of 47%, which is comparable with values from the current literature.

2. System Description

We consider a multipartite system, comprised of a transmon qubit of tunable frequency ω_{T}, which interacts with a transmission line (cavity) of natural frequency ω_{CPW} with coupling strength g. The cavity is pumped by an external field of amplitude E_d and single frequency ω (see Figure 1). Both systems are in contact with a classical heat bath at temperature T. Such a set-up is experimentally realistic and several implementations have already been reported in different contexts [28,33]. Here and in the following, the transmon is used as a working substance (WS) and the (non-standard) "bath" is represented by the net effect of the other two systems: the cavity and the cryogenic environment (classical bath). There are two subtleties that must be noted here: (i) the bath "seen" by the qubit does not only consist of a classical reservoir at some fixed temperature, but it has an additional component, namely the pumped cavity. By changing the pumping, several cavity states can be realized. Such a feature gives the possibility of making this composed bath *non-thermal* on demand. In addition, (ii), the proposed engine is devised as containing only one bath (cavity + environment), which does not pose any problems considering that it is an out-of-equilibrium bath.

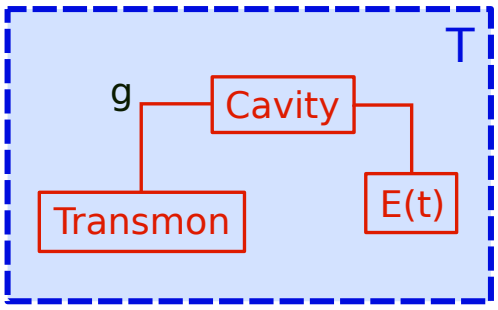

Figure 1. Sketch of the quantum engine with a transmon qubit as working substance interacting with an externally pumped (E(t)) transmission line (cavity). Both systems are embedded in the same cryogenic environment, which plays the role of a standard thermal bath of temperature T. Such a setup gives a dynamics of a working substance in the presence of a controllable *non-thermal* environment.

We start our analysis from the Hamiltonian describing a tunable qubit interacting with a single mode pumped cavity through a Jaynes-Cummings interaction

$$\begin{aligned} H(t) = &\frac{\hbar\omega_{\mathrm{T}}}{2}\sigma_z + \hbar\omega_{\mathrm{CPW}}a^\dagger a + g\sigma_x(a + a^\dagger) \\ &+ E_d\left(ae^{i\omega t} + a^\dagger e^{-i\omega t}\right), \end{aligned} \tag{1}$$

where σ_x and σ_z are the Pauli matrices, $a^\dagger$ and a are the canonical bosonic creation and annihilation operators associated with the cavity excitations, g is the qubit-cavity coupling strength. The last term represents a monochromatic pumping of amplitude E_d and frequency ω applied to the cavity.

The experimental characterization of the qubit-cavity dissipative dynamics emerging from their interaction with the same thermal bath shows that the system's steady state is determined by the master equation [28]

$$\begin{aligned}\dot{\rho}(t) = &-\frac{i}{\hbar}[H_{\mathrm{RWA}}, \rho] + K^{-}_{\mathrm{CPW}}\mathcal{D}[a]\rho \\ &+ K^{+}_{\mathrm{CPW}}\mathcal{D}[a^{\dagger}]\rho + \Gamma^{-}\mathcal{D}[\sigma^{-}]\rho + \Gamma^{+}\mathcal{D}[\sigma^{+}]\rho,\end{aligned} \tag{2}$$

with $K^{-}_{\mathrm{CPW}}(K^{+}_{\mathrm{CPW}})$ being the cavity decay (excitation) rate, $\Gamma^{-}(\Gamma^{+})$ the qubit relaxation (excitation) rate and $\mathcal{D}[A]\rho = A\rho A^{\dagger} - 1/2(A^{\dagger}A\rho + \rho A^{\dagger}A)$. Please note that these rates satisfy detailed balance for the same bath of temperature T, $K^{+}_{\mathrm{CPW}}/K^{-}_{\mathrm{CPW}} = \exp\left(-\hbar\omega_{\mathrm{CPW}}/k_{\mathrm{B}}T\right)$ and $\Gamma^{+}/\Gamma^{-} = \exp\left(-\hbar\omega_{\mathrm{T}}/k_{\mathrm{B}}T\right)$. The Hamiltonian part

$$\begin{aligned}H_{\mathrm{RWA}} = &\frac{\hbar}{2}\left(\omega_{\mathrm{T}} - \omega\right)\sigma_{z} + \hbar\left(\omega_{\mathrm{CPW}} - \omega\right)a^{\dagger}a \\ &+ g(\sigma_{+}a + \sigma_{-}a^{\dagger}) + E_{d}(a + a^{\dagger}),\end{aligned} \tag{3}$$

is the system Hamiltonian in the rotating wave approximation (RWA) [34], with $\sigma_{+}(\sigma_{-})$ being the spin ladder operators.

Since we are interested in the observed dynamics of the WS, it is necessary to find the qubit's reduced density matrix $\rho_{\mathrm{T}}(t) \equiv \mathrm{tr}_{\mathrm{a}}\left\{\rho(t)\right\}$, where $\mathrm{tr}_{\mathrm{a}}\left\{\cdot\right\}$ represents the partial trace on the cavity's degrees of freedom. The system state is in a qubit-cavity product state, i.e., $\rho(t) \approx \rho_{\mathrm{T}}(t) \otimes \rho_{\mathrm{C}}(t)$, which emerges in the effective qubit-cavity weak coupling regime due to decoherence into the global environment. In addition, the cavity's stationary state $\rho_{\mathrm{C}}(t)$ is assumed to be mainly determined by the external pumping, which can be easily found for situations of strong pumping and/or weak coupling strength g. This closely resembles a situation, in which the cavity acts as a work source of effectively infinite inertia [35]. Thus, changing the state of the qubit does not affect the state of the cavity, but it is still susceptible to the applied field and the cryogenic bath, and we have

$$\langle a\rangle = \langle a^{\dagger}\rangle^{*} = \frac{E_{d}}{\hbar\left[i\kappa_{\mathrm{CPW}}/2 - \left(\omega_{\mathrm{CPW}} - \omega\right)\right]}, \tag{4}$$

where we defined $K^{-}_{\mathrm{CPW}} = \kappa_{\mathrm{CPW}}$. Hence, the reduced master equation (2) can be written as

$$\dot{\rho}_{\mathrm{T}}(t) = -\frac{i}{\hbar}[\tilde{H}_{\mathrm{T,RWA}}, \rho_{\mathrm{T}}] + \Gamma^{-}\mathcal{D}[\sigma^{-}]\rho_{\mathrm{T}} + \Gamma^{+}\mathcal{D}[\sigma^{+}]\rho_{\mathrm{T}}, \tag{5}$$

with

$$\tilde{H}_{\mathrm{T,RWA}} = \frac{\hbar}{2}(\omega_{\mathrm{T}} - \omega)\sigma_{z} + g\left[\langle a\rangle\sigma_{+} + \langle a^{\dagger}\rangle\sigma_{-}\right]. \tag{6}$$

Please note that the effective qubit Hamiltonian carries information about the interaction with the cavity through $\langle a\rangle$ and $\langle a^{\dagger}\rangle$, which are dependent on the cavity state.

3. Non-Equilibrium Thermodynamics

3.1. Non-Thermal Equilibrium States

The only processes that are fully describable by means of conventional thermodynamics are infinitely slow successions of equilibrium states. For the operating principles of heat engines, the second law states that the maximum attainable efficiency of a thermal engine operating between two heat baths is limited by Carnot's efficiency.

An extension of this standard description is considering infinitely slow successions along *non-Gibbsian*, but stationary states [4,18–20,36]. In the present case, namely a heat engine with transmon qubit as working substance, non-Gibbsianity is induced by the external excitation applied as a driving

field to the cavity. We will see in the following, however, that identifying the thermodynamic work is subtle – and that the energy exchange can exhibit heat-like character, which is crucial when computing the entropy variation during the engine operation.

The stationary state can be found by solving the master equation Equation (5), and is written as

$$\rho_{\mathrm{T}}^{ss} = \begin{pmatrix} \rho_{\mathrm{T}}^{ee} & \rho_{\mathrm{T}}^{eg} \\ \rho_{\mathrm{T}}^{ge} & \rho_{\mathrm{T}}^{gg} \end{pmatrix} \tag{7}$$

where the matrix elements can be computed explicitly and are summarized in Appendix A.

We observe that for the case of effective qubit-cavity ultra-weak coupling, i.e., $\hbar\omega_{\mathrm{T}} \gg gE_d/\left|i\hbar\kappa_{\mathrm{CPW}}/2 - \hbar(\omega_{\mathrm{CPW}} - \omega)\right|$, as expected, the obtained non-thermal state asymptotically approaches thermal equilibrium, namely $|\rho_{\mathrm{T}}^{eg}| = |\rho_{\mathrm{T}}^{ge}| \approx 0$ and $\rho_{\mathrm{T}}^{ee}/\rho_{\mathrm{T}}^{gg} \approx \exp\left(-\beta\hbar\omega_{\mathrm{T}}\right)$. In addition, as also expected, in the high temperature limit $\hbar\omega_{\mathrm{T}}/kT \ll 1$ the qubit stationary state becomes the thermal, maximally mixed state, given that the cavity is not strongly pumped.

3.2. The Cycle

In equilibrium thermodynamics cycles are constructed by following a closed path on a surface obtained by the equation of state [29], which characterizes possible equilibrium states for a given set of macroscopic variables. This procedure can be generalized in the context of steady state thermodynamics, where an equation of state is also constructed.

For the present purposes, we use the steady state (7) to devise a cycle for our heat engine. The equation of state in our case is represented by the stationary state's von Neumann entropy $S(\omega_{\mathrm{T}}, E_d) = -\mathrm{tr}\left\{\rho_{\mathrm{T}}^{ss} \ln \rho_{\mathrm{T}}^{ss}\right\}$, which is fully determined by the pair of controllable variables ω_{T}, the transmon's frequency, and E_d, amplitude field of the pumping applied to the cavity. In order to implement the cycle, the stationary state is slowly varied (quasi-static) (The timescale for which the changes made can be considered slow is such that the conditions imposed to the system state are satisfied, namely the state is a product state and the cavity steady state is a coherent state with Equation (4)) by changing the "knobs" $(\omega_{\mathrm{T}}, E_d)$. It is composed of four strokes where we keep one of the two controllable variables constant and vary the other one, for example, at the first stroke we keep $E_d = E_0$ and vary ω_{T} from ω_0 to ω_1. The complete cycle is sketched in Figure 2.

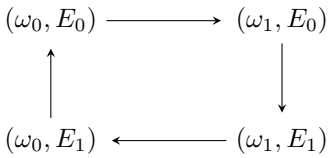

Figure 2. Sketch of the thermodynamic cycle obtained by varying the tunable parameters ω_{T} and E_d. Each one of the strokes are obtained by keeping one of the variables constant while quasi-statically varying the other one.

Since we are interested in analyzing the engine as a function of its parameters of operation, we simulated several cycles with boundary values (ω_1, E_1), which will range from the minimum value (ω_0, E_0) to the maximum one $(\omega_{1,\max}, E_{1,\max})$. The corresponding cycles lie on the von Neumann entropy surface depicted in Figure 3. In Appendix A plots of the stationary state's population and quantum coherence ρ_{T}^{ee} and $|\rho_{\mathrm{T}}^{eg}|$ as a function of $(\omega_{\mathrm{T}}, E_d)$ are shown. There we can observed clearly that the WS exhibits quantum coherence and population changes during its operation.

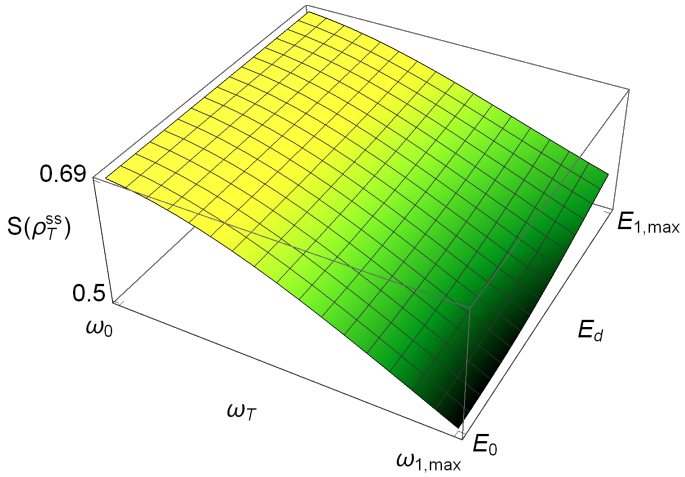

Figure 3. Stationary state's von Neumann entropy in the regime of operation of the thermal engine. Any thermodynamic cycle must be contained on this surface.

Finally, it is worth emphasizing that in the present analysis all parameters were chosen from an *experimentally accessible* regime [28,30–32], under the validity of the approximation of weak-coupling interaction between transmon and cavity. The parameters are collected in Table 1.

Table 1. Engine parameters used in the present analysis.

Parameter	Value
$\omega_{\mathrm{CPW}}/2\pi$	4.94 GHz
$\omega/2\pi$	4.94 GHz
$g/2\pi\hbar$	120 MHz
T	30 mK
$\Gamma/2\pi$	2 MHz
$\kappa_{\mathrm{CPW}}/2\pi$	1 MHz
$\omega_0/2\pi$	100 MHz
$\omega_{1,\mathrm{max}}/2\pi$	1000 MHz
$E_0/2\pi\hbar$	0.2 MHz
$E_{1,\mathrm{max}}/2\pi\hbar$	2 MHz

4. Work, Heat and Efficiency

The first law of thermodynamics, $\Delta E(t) = W(t) + Q(t)$, states that a variation of the internal energy along a thermodynamic process can be divided into two different parts, work $W(t)$ and heat $Q(t)$, where for Lindblad dynamics we have [4,37],

$$\begin{aligned} W(t) &= \int_0^t \mathrm{tr}\left\{\rho(t')\dot{H}(t')dt'\right\}, \\ Q(t) &= \int_0^t \mathrm{tr}\left\{\dot{\rho}(t')H(t')dt'\right\}. \end{aligned} \tag{8}$$

Typically, work is understood as a controllable energy exchange, which can be used for something useful, while heat cannot be controlled, emerging from the unavoidable interaction of the engine with its environment. As stated before, there are certain situations in which it can be shown that part of $Q(t)$ does not cause any entropic variation [24]. This has led to proposals for the differentiation of two distinct forms of energy contributions to Q: the *passive energy* $\mathcal{Q}(t)$, which is responsible for the variation in entropy, and the variation in *ergotropy* $\Delta\mathcal{W}(t)$ which is a "work-like energy" that can

be extracted by means of a unitary transformation and consequently would not cause any entropic change. Both terms are defined as,

$$\begin{aligned} \mathcal{Q}(t) &= \int_0^t \mathrm{tr}\left\{\dot{\pi}(t')H(t')dt'\right\}, \\ \Delta\mathcal{W}(t) &= \int_0^t \mathrm{tr}\left\{[\dot{\rho}(t') - \dot{\pi}(t')]H(t')dt'\right\}, \end{aligned} \tag{9}$$

with $\pi(t)$ being the passive state [25] associated with the state $\rho(t)$ at time t. To calculate the upper bound on the efficiency for systems that exhibit these different "flavors" of energy one should replace Q by $\mathcal{Q}$ in statements of the second law, since the *ergotropy* is essentially a mechanical type of energy, and consequently not limited by the second law, resulting in a different upper bound, see also Ref. [24].

Distinguishing these types of energy exchanged with the environment is crucial when one is interested in determining the fundamental upper bounds on the efficiency. However, in the present context, we are more interested in experimentally relevant statements, i.e., computing the efficiency in terms of what can be measured directly. Thus, we consider the ratio of the extracted work to the total energy acquired from the bath, independent of its type [24].

The cycle designed here is such that in each stroke one of the knobs $(\omega_{\mathrm{T}}, E_d)$ is kept fixed, while the other one is changed. Recall that the cavity is assumed to be a subpart of the bath seen by the WS, and that its state is modified by E_d. Since the WS is always in contact with the environment, one has that heat and work are exchanged in each stroke. Here, such a calculation is done by using Equation (8), considering the stationary state Equation (7) and the effective WS Hamiltonian Equation (6). Then, for the ith stroke, the corresponding W_i and Q_i integrals, representing the work and heat delivered (extracted) to (from) the WS, can be parametrized in terms of the respective knob variation as we can see in Appendix B. These quantities are obtained using the WS effective Hamiltonian $\tilde{H}_{\mathrm{T,RWA}}$, which already takes into account the interaction with the external bath and pumped cavity.

Once these quantities are determined, we can calculate the efficiency η of this engine, defined by

$$\eta = -\frac{\sum_{i=1}^{4} W_i}{Q_+}, \tag{10}$$

with the delivered heat to the WS in a complete cycle being given by $Q_+ = \sum_{i=1}^{4} Q_+^i$, with Q_+^i the given heat (only positive contributions inside the stroke) during the i_{th} stroke (see Appendix B). Therefore, this efficiency represents the amount of work extracted from the engine through the use of the delivered heat to the WS.

Figure 4 shows the engine efficiency η attained in the execution of the strokes as a function of the boundary values (ω_1, E_1), as depicted in Figure 2. Please note that (ω_1, E_1) sweeps the entire spectrum of the tunable parameters $(\omega_{\mathrm{T}}, E_d)$, going from (ω_0, E_0) to $(\omega_{1,\mathrm{max}}, E_{1,\mathrm{max}})$ where we find the maximal efficiency. It is worth mentioning here that the highest value of the efficiency is dependent on the chosen regime of parameters, which in our case is based on experimentally attainable values [28,30–32]. As usual, in order to extract the predicted work, one has to couple our engine to another system. We envision using the experimental setup of Ref. [28], where a mechanical nanoresonator is present and weakly driven by the transmon. Thus, under such a configuration, by following the nanoresonator's state (recall that we have assumed infinite inertia, i.e., the transmon is not capable of changing the cavity's state. In situations where such an assumption does not hold, one has to take into account the possibility of having the transmon doing work on the cavity), one can determine the amount of energy transferred in the form of work. In addition, by observing the transmon's state, one can obtain the amount of heat given by the non-standard bath, providing a full characterization of our engine.

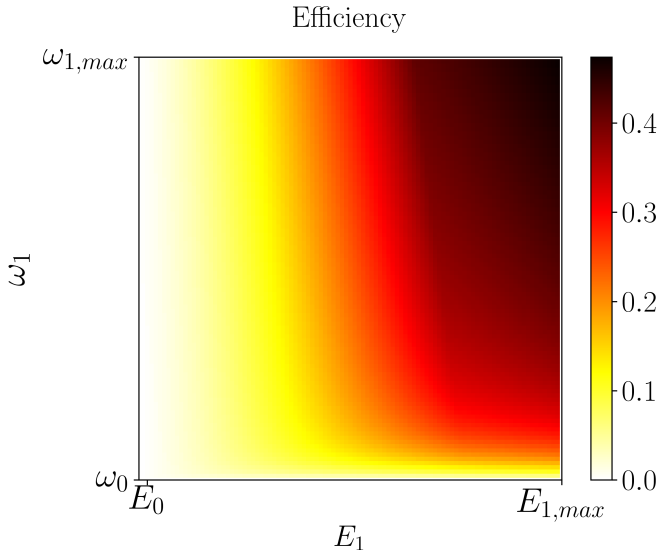

Figure 4. Efficiency η as a function of the upper values (ω_1, E_1) for the cycle depicted in Figure 2. The observed highest efficiency of about 47% was attained when $(\omega_1, E_1) = (\omega_{1,\max}, E_{1,\max})$, with $\omega_{1,\max}/2\pi = 1000$ MHz and $E_{1,\max}/2\pi\hbar = 2$ MHz.

5. Conclusions and Final Remarks

Theoretical research of small heat engines in the quantum domain is common place in quantum thermodynamics [37–46]. In the present work, we have devised a transmon-based heat engine using an experimentally realistic regime of parameters reaching a maximal efficiency of 47%, which turns out to be a reasonable value when compared with the state of the art in quantum heat engines. One of the most recent experiments in quantum heat engine was implemented by Peterson et al. [47] using a spin $-1/2$ system and nuclear resonance techniques, performing an Otto cycle with efficiency in excess of 42% at maximum power. It is important to stress that implementing small heat engines constitutes a hard task, even when dealing with classical systems. Indeed, a representative example is the single ion confined in a linear Paul trap with a tapered geometry, which was used to implement a Stirling engine [48] with efficiency of only 0.28%. Additional research is being carried out concerning the behavior of this engine influenced by the presence of coherence and the dimension of the WS. By devising this theoretical protocol for the implementation of a quantum engine, we hope to help the community, and in particular experimentalists, in the formidable task to design and implement quantum thermodynamic systems and to consolidate the concepts of this new exiting field of research.

Author Contributions: C.C., F.B. and S.D. equally contributed to conceptualization, investigation and writing of the paper.

Funding: C.C. and F.B. acknowledge financial support in part by the Coordenação de Aperfeiçoamento de Pessoal de Nível Superior—Brasil (CAPES)—Finance Code 001. During his stay at UMBC, C.C. was supported by the CAPES scholarship PDSE/process No. 88881.132982/2016-01. F.B. is also supported by the Brazilian National Institute for Science and Technology of Quantum Information (INCT-IQ) under Grant No. 465469/2014-0/CNPq. S.D. acknowledges support from the U.S. National Science Foundation under Grant No. CHE-1648973.

Acknowledgments: We thank F. Rouxinol and V. F. Teizen for valuable discussions. C.C. would like to thank the hospitality of UMBC, where most of this research was conducted.

Conflicts of Interest: The authors declare no conflict of interest.

Appendix A. Non-Thermal Equilibrium States

Here, we summarize the explicit expressions of the density matrix elements of ρ_{T}^{ss} (7), which are plotted as a function of $(\omega_{\mathrm{T}}, E_{\mathrm{d}})$ in Figure A1 .

$$\rho_{\mathrm{T}}^{ee} = \frac{\frac{g^2E_d^2}{\hbar^4\left[\frac{1}{4}\kappa_{\mathrm{CPW}}^2+(\omega_{\mathrm{CPW}}-\omega)^2\right]} + \frac{1}{1+e^{\beta\hbar\omega_{\mathrm{T}}}}\left[\frac{1}{4}\frac{\Gamma^2}{\tanh^2(\beta\hbar\omega_{\mathrm{T}}/2)} + (\omega_{\mathrm{T}}-\omega)^2\right]}{\frac{2g^2E_d^2}{\hbar^4\left[\frac{1}{4}\kappa_{\mathrm{CPW}}^2+(\omega_{\mathrm{CPW}}-\omega)^2\right]} + \left[\frac{1}{4}\frac{\Gamma^2}{\tanh^2(\beta\hbar\omega_{\mathrm{T}}/2)} + (\omega_{\mathrm{T}}-\omega)^2\right]}, \tag{A1}$$

$$\rho_{\mathrm{T}}^{gg} = \frac{\frac{g^2E_d^2}{\hbar^4\left[\frac{1}{4}\kappa_{\mathrm{CPW}}^2+(\omega_{\mathrm{CPW}}-\omega)^2\right]} + \frac{1}{1+e^{-\beta\hbar\omega_{\mathrm{T}}}}\left[\frac{1}{4}\frac{\Gamma^2}{\tanh^2(\beta\hbar\omega_{\mathrm{T}}/2)} + (\omega_{\mathrm{T}}-\omega)^2\right]}{\frac{2g^2E_d^2}{\hbar^4\left[\frac{1}{4}\kappa_{\mathrm{CPW}}^2+(\omega_{\mathrm{CPW}}-\omega)^2\right]} + \left[\frac{1}{4}\frac{\Gamma^2}{\tanh^2(\beta\hbar\omega_{\mathrm{T}}/2)} + (\omega_{\mathrm{T}}-\omega)^2\right]}, \tag{A2}$$

$$\rho_{\mathrm{T}}^{eg} = \frac{\frac{1}{2\hbar}\left[\frac{\Gamma}{\tanh(\beta\hbar\omega_{\mathrm{T}}/2)}i + 2(\omega_{\mathrm{T}}-\omega)\right]\frac{gE_d}{\hbar\left[i\frac{\kappa_{\mathrm{CPW}}}{2}-(\omega_{\mathrm{CPW}}-\omega)\right]}}{\frac{2g^2E_d^2}{\hbar^4\left[\frac{1}{4}\kappa_{\mathrm{CPW}}^2+(\omega_{\mathrm{CPW}}-\omega)^2\right]} + \left[\frac{1}{4}\frac{\Gamma^2}{\tanh^2(\beta\hbar\omega_{\mathrm{T}}/2)} + (\omega_{\mathrm{T}}-\omega)^2\right]}\tanh(\beta\hbar\omega_{\mathrm{T}}/2). \tag{A3}$$

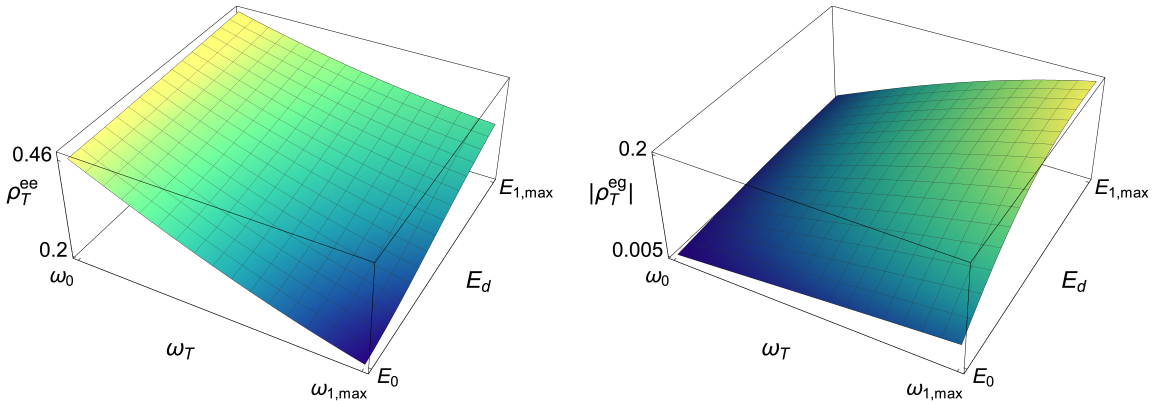

Figure A1. Stationary state's elements ρ_{T}^{ee} and $|\rho_{\mathrm{T}}^{eg}|$ for different values of $(\omega_{\mathrm{T}}, E_d)$. Important amounts of population and quantum coherence changes can be reached during the engine operation.

Appendix B. Thermodynamic Quantities along Each Stroke

In this appendix we summarize the explicit expressions of the thermodynamic quantities W_i and Q_i for $i = 1, 2, 3, 4$ and the heat Q_+ given to the WS. These quantities are obtained by changing quasi-statically the parameters ω_{T} and E_d producing a succession of steady states $\hat{\rho}_{\mathrm{T}}^{ss}(\omega_{\mathrm{T}}, E_d)$:

$$\begin{aligned}
W_1 &= \int_{\omega_0}^{\omega_1} \mathrm{tr}\left\{\hat{\rho}_{\mathrm{T}}^{ss}(\omega_{\mathrm{T}}, E_0)\left(\frac{\partial\tilde{H}_{\mathrm{T,RWA}}}{\partial\omega_{\mathrm{T}}}\right)_{E_0}\right\} d\omega_{\mathrm{T}},\\
W_2 &= \int_{E_0}^{E_1} \mathrm{tr}\left\{\hat{\rho}_{\mathrm{T}}^{ss}(\omega_1, E_d)\left(\frac{\partial\tilde{H}_{\mathrm{T,RWA}}}{\partial E_d}\right)_{\omega_1}\right\} dE_d,\\
W_3 &= \int_{\omega_1}^{\omega_0} \mathrm{tr}\left\{\hat{\rho}_{\mathrm{T}}^{ss}(\omega_{\mathrm{T}}, E_1)\left(\frac{\partial\tilde{H}_{\mathrm{T,RWA}}}{\partial\omega_{\mathrm{T}}}\right)_{E_1}\right\} d\omega_{\mathrm{T}},\\
W_4 &= \int_{E_1}^{E_0} \mathrm{tr}\left\{\hat{\rho}_{\mathrm{T}}^{ss}(\omega_0, E_d)\left(\frac{\partial\tilde{H}_{\mathrm{T,RWA}}}{\partial E_d}\right)_{\omega_0}\right\} dE_d.
\end{aligned} \tag{A4}$$

$$
\begin{aligned}
Q_1 &= \int_{\omega_0}^{\omega_1} \mathrm{tr}\left\{\left(\frac{\partial\hat{\rho}_{\mathrm{T}}^{ss}}{\partial\omega_{\mathrm{T}}}\right)_{E_0} \tilde{H}_{\mathrm{T,RWA}}(\omega_{\mathrm{T}}, E_0)\right\} d\omega_{\mathrm{T}},\\
Q_2 &= \int_{E_0}^{E_1} \mathrm{tr}\left\{\left(\frac{\partial\hat{\rho}_{\mathrm{T}}^{ss}}{\partial E_d}\right)_{\omega_1} \tilde{H}_{\mathrm{T,RWA}}(\omega_1, E_d)\right\} dE_d,\\
Q_3 &= \int_{\omega_1}^{\omega_0} \mathrm{tr}\left\{\left(\frac{\partial\hat{\rho}_{\mathrm{T}}^{ss}}{\partial\omega_{\mathrm{T}}}\right)_{E_1} \tilde{H}_{\mathrm{T,RWA}}(\omega_{\mathrm{T}}, E_1)\right\} d\omega_{\mathrm{T}},\\
Q_4 &= \int_{E_1}^{E_0} \mathrm{tr}\left\{\left(\frac{\partial\hat{\rho}_{\mathrm{T}}^{ss}}{\partial E_d}\right)_{\omega_0} \tilde{H}_{\mathrm{T,RWA}}(\omega_0, E_d)\right\} dE_d.
\end{aligned} \tag{A5}
$$

$$
Q_+ = \sum_{i=1}^{4} Q_+^i \tag{A6}
$$

with Q_+^i for $i = 1, 2, 3, 4$ given by

$$
\begin{aligned}
Q_+^1 &= \int_{\omega_0}^{\omega_1} \mathrm{tr}\left\{\left(\frac{\partial\hat{\rho}_{\mathrm{T}}^{ss}}{\partial\omega_{\mathrm{T}}}\right)_{E_0} \tilde{H}_{\mathrm{T,RWA}}(\omega_{\mathrm{T}}, E_0)\right\} \Theta\left[\mathrm{tr}\left\{\left(\frac{\partial\hat{\rho}_{\mathrm{T}}^{ss}}{\partial\omega_{\mathrm{T}}}\right)_{E_0} \tilde{H}_{\mathrm{T,RWA}}(\omega_{\mathrm{T}}, E_0)\right\} d\omega_{\mathrm{T}}\right],\\
Q_+^2 &= \int_{E_0}^{E_1} \mathrm{tr}\left\{\left(\frac{\partial\hat{\rho}_{\mathrm{T}}^{ss}}{\partial E_d}\right)_{\omega_1} \tilde{H}_{\mathrm{T,RWA}}(\omega_1, E_d)\right\} \Theta\left[\mathrm{tr}\left\{\left(\frac{\partial\hat{\rho}_{\mathrm{T}}^{ss}}{\partial E_d}\right)_{\omega_1} \tilde{H}_{\mathrm{T,RWA}}(\omega_1, E_d)\right\} dE_d\right],\\
Q_+^3 &= \int_{\omega_1}^{\omega_0} \mathrm{tr}\left\{\left(\frac{\partial\hat{\rho}_{\mathrm{T}}^{ss}}{\partial\omega_{\mathrm{T}}}\right)_{E_1} \tilde{H}_{\mathrm{T,RWA}}(\omega_{\mathrm{T}}, E_1)\right\} \Theta\left[\mathrm{tr}\left\{\left(\frac{\partial\hat{\rho}_{\mathrm{T}}^{ss}}{\partial\omega_{\mathrm{T}}}\right)_{E_1} \tilde{H}_{\mathrm{T,RWA}}(\omega_{\mathrm{T}}, E_1)\right\} d\omega_{\mathrm{T}}\right],\\
Q_+^4 &= \int_{E_1}^{E_0} \mathrm{tr}\left\{\left(\frac{\partial\hat{\rho}_{\mathrm{T}}^{ss}}{\partial E_d}\right)_{\omega_0} \tilde{H}_{\mathrm{T,RWA}}(\omega_0, E_d)\right\} \Theta\left[\mathrm{tr}\left\{\left(\frac{\partial\hat{\rho}_{\mathrm{T}}^{ss}}{\partial E_d}\right)_{\omega_0} \tilde{H}_{\mathrm{T,RWA}}(\omega_0, E_d)\right\} dE_d\right].
\end{aligned} \tag{A7}
$$

where the Heaviside function $\Theta[\cdot]$ is inside the integral, selecting only the positive contributions (heat given to the WS) along the stroke.

References

1. Gemmer, J.; Michel, M.; Mahler, G. *Quantum Thermodynamics*; Springer: Berlin/Heidelberg, Germany, 2004.
2. Gelin, M.F.; Thoss, M. Thermodynamics of a subensemble of a canonical ensemble. *Phys. Rev. E* **2009**, *79*, 051121. [CrossRef]
3. Scully, M.O.; Zubairy, M.S.; Agarwal, G.S.; Walther, H. Extracting Work from a Single Heat Bath via Vanishing Quantum Coherence. *Science* **2003**, *299*, 862. [CrossRef] [PubMed]
4. Gardas, B.; Deffner, S. Thermodynamic universality of quantum Carnot engines. *Phys. Rev. E* **2015**, *92*, 042126. [CrossRef] [PubMed]
5. Deffner, S. Efficiency of Harmonic Quantum Otto Engines at Maximal Power. *Entropy* **2018**, *20*, 875. [CrossRef]
6. Çakmak, B.; Müstecaplıoğlu, O.E. Spin quantum heat engines with shortcuts to adiabaticity. *Phys. Rev. E* **2019**, *99*, 032108. [CrossRef]
7. Klaers, J.; Faelt, S.; Imamoglu, A.; Togan, E. Squeezed Thermal Reservoirs as a Resource for a Nanomechanical Engine beyond the Carnot Limit. *Phys. Rev. X* **2017**, *7*, 031044. [CrossRef]
8. Dillenschneider, R.; Lutz, E. Energetics of quantum correlations. *EPL (Europhys. Lett.)* **2009**, *88*, 50003. [CrossRef]
9. Huang, X.L.; Wang, T.; Yi, X.X. Effects of reservoir squeezing on quantum systems and work extraction. *Phys. Rev. E* **2012**, *86*, 051105. [CrossRef] [PubMed]
10. Abah, O.; Lutz, E. Efficiency of heat engines coupled to nonequilibrium reservoirs. *EPL (Europhys. Lett.)* **2014**, *106*, 20001. [CrossRef]
11. Roßnagel, J.; Abah, O.; Schmidt-Kaler, F.; Singer, K.; Lutz, E. Nanoscale Heat Engine Beyond the Carnot Limit. *Phys. Rev. Lett.* **2014**, *112*, 030602. [CrossRef]
12. Hardal, A.Ü.C.; Müstecaplıoğlu, Ö.E. Superradiant Quantum Heat Engine. *Sci. Rep.* **2015**, *5*, 12953. [CrossRef]
13. Niedenzu, W.; Gelbwaser-Klimovsky, D.; Kofman, A.G.; Kurizki, G. On the operation of machines powered by quantum non-thermal baths. *New J. Phys.* **2016**, *18*, 083012. [CrossRef]

14. Manzano, G.; Galve, F.; Zambrini, R.; Parrondo, J.M.R. Entropy production and thermodynamic power of the squeezed thermal reservoir. *Phys. Rev. E* **2016**, *93*, 052120. [CrossRef]
15. Agarwalla, B.K.; Jiang, J.H.; Segal, D. Quantum efficiency bound for continuous heat engines coupled to noncanonical reservoirs. *Phys. Rev. B* **2017**, *96*, 104304. [CrossRef]
16. Stefanatos, D. Optimal efficiency of a noisy quantum heat engine. *Phys. Rev. E* **2014**, *90*, 012119. [CrossRef]
17. Torrontegui, E.; Kosloff, R. Quest for absolute zero in the presence of external noise. *Phys. Rev. E* **2013**, *88*, 032103. [CrossRef]
18. Gardas, B.; Deffner, S.; Saxena, A. Non-hermitian quantum thermodynamics. *Sci. Rep.* **2016**, *6*, 23408. [CrossRef]
19. Hatano, T.; Sasa, S.I. Steady-State Thermodynamics of Langevin Systems. *Phys. Rev. Lett.* **2001**, *86*, 3463. [CrossRef]
20. Oono, Y.; Paniconi, M. Steady State Thermodynamics. *Prog. Theor. Phys. Suppl.* **1998**, *130*, 29. [CrossRef]
21. Horowitz, J.M.; Sagawa, T. Equivalent Definitions of the Quantum Nonadiabatic Entropy Production. *J. Stat. Phys.* **2014**, *156*, 55. [CrossRef]
22. Yuge, T.; Sagawa, T.; Sugita, A.; Hayakawa, H. Geometrical Excess Entropy Production in Nonequilibrium Quantum Systems. *J. Stat. Phys.* **2013**, *153*, 412. [CrossRef]
23. Binder, F.; Vinjanampathy, S.; Modi, K.; Goold, J. Quantum thermodynamics of general quantum processes. *Phys. Rev. E* **2015**, *91*, 032119. [CrossRef]
24. Niedenzu, W.; Mukherjee, V.; Ghosh, A.; Kofman, A.G.; Kurizki, G. Quantum engine efficiency bound beyond the second law of thermodynamics. *Nat. Commun.* **2018**, *9*, 165. [CrossRef]
25. Pusz, W.; Woronowicz, S.L. Passive states and KMS states for general quantum systems. *Commun. Math. Phys.* **1978**, *58*, 273. [CrossRef]
26. Allahverdyan, A.E.; Balian, R.; Nieuwenhuizen, T.M. Maximal work extraction from finite quantum systems. *EPL (Europhys. Lett.)* **2004**, *67*, 565. [CrossRef]
27. Manzano, G. Squeezed thermal reservoir as a generalized equilibrium reservoir. *Phys. Rev. E* **2018**, *98*, 042123. [CrossRef]
28. Rouxinol, F.; Hao, Y.; Brito, F.; Caldeira, A.O.; Irish, E.K.; LaHaye, M.D. Measurements of nanoresonator-qubit interactions in a hybrid quantum electromechanical system. *Nanotechnology* **2016**, *27*, 364003. [CrossRef]
29. Callen, H.B. *Thermodynamics and an Introduction to Thermostatistics*; Wiley: Hoboken, NJ, USA, 1985.
30. Kok, P.; Munro, W.J.; Nemoto, K.; Ralph, T.C.; Dowling, J.P.; Milburn, G.J. Linear optical quantum computing with photonic qubits. *Rev. Mod. Phys.* **2007**, *79*, 135. [CrossRef]
31. Hofheinz, M.; Weig, E.M.; Ansmann, M.; Bialczak, R.C.; Lucero, E.; Neeley, M.; O'Connell, A.D.; Wang, H.; Martinis, J.M.; Cleland, A.N. Generation of Fock states in a superconducting quantum circuit. *Nature* **2008**, *454*, 310. [CrossRef]
32. Mallet, F.; Ong, F.R.; Palacios-Laloy, A.; Nguyen, F.; Bertet, P.; Vion, D.; Esteve, D. Single-shot qubit readout in circuit Quantum Electrodynamics. *Nat. Phys.* **2009**, *5*, 791. [CrossRef]
33. Majer, J.; Chow, J.M.; Gambetta, J.M.; Koch, J.; Johnson, B.R.; Schreier, J.A.; Frunzio, L.; Schuster, D.I.; Houck, A.A.; Wallraff, A.; et al. Coupling Superconducting Qubits via a Cavity Bus. *Nature* **2007**, *449*, 443. [CrossRef]
34. Scully, M.O.; Zubairy, M.S. *Quantum Optics*; Cambridge University Press: Cambridge, UK, 1997. [CrossRef]
35. Deffner, S.; Jarzynski, C. Information Processing and the Second Law of Thermodynamics: An Inclusive, Hamiltonian Approach. *Phys. Rev. X* **2013**, *3*, 041003. [CrossRef]
36. Sasa, S.I.; Tasaki, H. Steady State Thermodynamics. *J. Stat. Phys.* **2006**, *125*, 125. [CrossRef]
37. Alicki, R. The quantum open system as a model of the heat engine. *J. Phys. A Math. Gen.* **1979**, *12*, L103. [CrossRef]
38. Geva, E.; Kosloff, R. A quantum-mechanical heat engine operating in finite time. A model consisting of spin-1/2 systems as the working fluid. *J. Chem. Phys* **1998**, *96*, 3054. [CrossRef]
39. Kieu, T.D. The Second Law, Maxwell's Demon, and Work Derivable from Quantum Heat Engines. *Phys. Rev. Lett.* **2004**, *93*, 140403. [CrossRef] [PubMed]
40. Quan, H.T.; Liu, Y.X.; Sun, C.P.; Nori, F. Quantum thermodynamic cycles and quantum heat engines. *Phys. Rev. E* **2007**, *76*, 031105. [CrossRef]
41. Linden, N.; Popescu, S.; Skrzypczyk, P. How Small Can Thermal Machines Be? The Smallest Possible Refrigerator. *Phys. Rev. Lett.* **2010**, *105*, 130401. [CrossRef]

42. Correa, L.A.; Palao, J.P.; Alonso, D.; Adesso, G. Quantum-enhanced absorption refrigerators. *Sci. Rep.* **2014**, *4*, 3949. [CrossRef]
43. Uzdin, R.; Levy, A.; Kosloff, R. Equivalence of Quantum Heat Machines, and Quantum-Thermodynamic Signatures. *Phys. Rev. X* **2015**, *5*, 031044. [CrossRef]
44. Abah, O.; Roßnagel, J.; Jacob, G.; Deffner, S.; Schmidt-Kaler, F.; Singer, K.; Lutz, E. Single-Ion Heat Engine at Maximum Power. *Phys. Rev. Lett.* **2012**, *109*, 203006. [CrossRef]
45. Zhang, K.; Bariani, F.; Meystre, P. Quantum Optomechanical Heat Engine. *Phys. Rev. Lett.* **2014**, *112*, 150602. [CrossRef]
46. Dawkins, S.T.; Abah, O.; Singer, K.; Deffner, S. Single Atom Heat Engine in a Tapered Ion Trap. In *Thermodynamics in the Quantum Regime: Fundamental Aspects and New Directions*; Binder, F., Correa, L.A., Gogolin, C., Anders, J., Adesso, G., Eds.; Springer International Publishing: Cham, Switzerland, 2018; pp. 887–896. [CrossRef]
47. Peterson, J.P.S.; Batalhão, T.B.; Herrera, M.; Souza, A.M.; Sarthour, R.S.; Oliveira, I.S.; Serra, R.M. Experimental characterization of a spin quantum heat engine. *arXiv* **2018**, arXiv:1803.06021.
48. Roßnagel, J.; Dawkins, S.T.; Tolazzi, K.N.; Abah, O.; Lutz, E.; Schmidt-Kaler, F.; Singer, K. A single-atom heat engine. *Science* **2016**, *352*, 325. [CrossRef]